JOURNAL OF MATERIALS SCIENCE 10 (1975) 1959–1970

The annealing of solution-crystallized polyethylene mats: an X-ray diffraction study

A. H. WINDLE
Department of Metallurgy and Materials Science, Imperial College of Science and Technology, London, UK

Both low- and wide-angle X-ray diffraction measurements have been made on solution-crystallized mats of high density polyethylene which have been annealed for different periods at 125° C. The low-angle data, in addition to showing the rapid increase in both long period and density defect at each fold surface for the first stages of annealing, also indicate that after annealing for times in excess of 10^5 sec the density defect is reduced and approaches the value for the unannealed crystal. The wide-angle X-ray studies have centred around the Fourier analysis of the 0 0 2 diffraction peak. The results of this type of measurement on unannealed mats have already been reported [20]. In extending the work to annealed material evidence has been obtained for preferred chain stem lengths which are multiples of the unannealed length. The combination of these observations with the low-angle results has led to the formulation of a model for crystal thickening which invokes the unlooping mechanism proposed by Dreyfuss and Keller [15], but also envisages thickening occurring preferentially from one fold surface to give an asymmetric crystal profile in the [0 0 1] direction.

1. Introduction

One year after the discovery in 1957 that polyethylene single crystals consisted of folded chains [1, 2], it was reported that the thickness of the crystals as measured by small-angle X-ray diffraction (the long period) could be increased by annealing close to the melting point [3]. Since that time several similar and more detailed observations of the effect of annealing polyethylene on its long period have been recorded [4, 5]. Thickening has been observed using transmission electron microscopy [6–8], and has also formed a basis of explanations of the effect of annealing on mechanical relaxation [9] and gas adsorption properties [10]. These last two papers also emphasise the marked difference in annealing behaviour between solution and melt-crystallized material.

In terms of molecular mechanisms it is not possible to consider annealing behaviour in isolation from the processes of crystallization and melting, and accordingly the range of current molecular models for these processes is reflected in a similar diversity of models to describe crystal thickening on annealing. It is generally agreed that the thickening must involve a specially high chain mobility at the annealing temperature – at least in the chain direction – but the question as to whether the high mobility is the result of transient melting remains open.

The observation of a double melting peak in differential scanning calorimetry traces [11] which is not seen if the sample is mildly irradiated [12] suggests that melting of the thin crystals is followed by their recrystallization as thicker, higher melting points entities. It is difficult, however, to reconcile complete, albeit transient, melting with the fact that the thickened crystals are of identical orientation to the original. On the other hand, several molecular mechanisms have been proposed to explain thickening which do not involve melting [13–15]. One of these was put forward by Dreyfuss and Keller [15] as the result of obser-

vations that the annealing of polyamides led to a doubling, and under some conditions a quadrupling, of the long period. It envisages the pulling out of individual folds which in addition to providing a neat explanation of the observed doubling could also account for the insensitivity of annealing behaviour to molecular weight noted in some instances [14].

Measurements of density changes on annealing have provided other clues as to the structural variations which may occur in the region of the fold surfaces. The density data of Fischer and Schmidt [16] and more recently of Blackadder and Lewell [17] showed that annealing polyethylene below 120° C leads to a gradual increase in density along with the fold period, whereas if annealing is carried out between 120° C and the melting point, there is an initial decrease in density followed by an increase after long times. Blackadder and Lewell further developed the suggestion of Bair *et al.* [12] that there are two annealing mechanisms, one predominant below 117° C and the other above. On the basis of measurements of tensile modulus, swelling due to solvent penetration, density and SAXD long periods, they proposed that the low temperature mechanism produces crystal thickening without any melting whereas that operating above 117° C involves partial melting.

Knowledge of the long period and the thickness of the completely crystalline components of the layers can provide an estimate of the thickness of the disordered layer. This approach was first applied to the annealing of polyethylene fibres by Statton [18] who showed that the thickness of the disordered layer increased with the crystal thickness. More recently Kobayashi and Keller [19] obtained values of the thickness of the disordered layer for solution crystallized polyethylene mats by subtracting the crystal thickness, obtained by measuring the half-width of the 0 0 2 peak, from the long period. They varied the long period by using different annealing treatments and observed that the disordered layer thickness was directly proportional to the long period.

2. Scope of this paper

This study is the direct extension of work already reported [19, 20] and was commenced at the instigation of Professor Keller in his laboratory. The specimens used for the annealing were cut from the same well-oriented crystalline mats of high density polyethylene prepared by Dr Kobayashi, and already studied in considerable detail by wide-angle X-ray diffraction.

The specimens were annealed for different periods at 125° C which is in the temperature range for which there is evidence of transient melting [12, 16, 17]. After the annealing treatment the specimens were rapidly cooled and their structure examined by quantitative small-angle X-ray diffraction and also by the analysis of the profile of the 0 0 2 peak – a technique already applied to unannealed specimens [20].

3. The specimens

3.1. Sample preparation and annealing

Specimens cut from the original mat of solution crystallized high density polyethylene (Rigidex 50) were annealed for different periods in a silicone oil bath maintained at 125 ± $\frac{1}{4}$° C, the specimens being brought to temperature by direct immersion in the bath and cooled by quenching in water. The two specimens annealed for the longest times (10^4 and 6×10^5 sec) were held between copper blocks in a test tube immersed in the bath so as to prevent any distortion of the specimen. Every attempt was made to reproduce the heating and cooling rates of the shorter anneals. The experimental results however tend to show a discontinuity in the gradual change in structure during annealing which is attributable to the change in technique. It may be the result of the sensitivity of annealing behaviour to small variations in heating and/or cooling rates even when the annealing period exceeds the time to reach the correct temperature by a factor of 10 000 or more. It is also possible that some degree of degradation due to oxygen occurred during the long anneals.

3.2. Preliminary survey of the structure

Both small- and wide-angle transmission X-ray diffraction photographs were prepared from the annealed specimens. The increase in long period was very apparent from the small-angle diffraction patterns and also caused a sharpening of some wide-angle reflection. The crystallographic texture was unchanged by annealing, the fold surfaces remaining perpendicular to the chain direction. There was some indication of a limited degree of broadening of the low-angle reflection in the direction of the layer lines on annealing which may suggest a reduction of the lateral dimensions of the crystals.

TABLE I

Specimen	Density
Unannealed	0.964
10 sec at 125° C	0.957
100 sec at 125° C	0.959
1100 sec at 125° C	0.965
10 000 sec at 125° C	0.970
600 000 sec at 125° C	0.985

3.3. Density measurements

The densities of annealed samples are summarized in Table I. They show the same trends as the data of Fischer and Schmidt [16], Blackadder and Lewell [17] and others for specimens annealed above about 120° C; namely, an initial decrease after short annealing times followed by an increase as annealing is prolonged. The subsequent density increase is particularly marked for the longest time at 125° C (6×10^5 sec).

4. Small-angle X-ray diffraction (SAXD)

4.1. Results and their interpretation

The SAXD patterns were recorded using a Kratky (slit collimated) camera. The data were corrected for background scattering and are plotted as the first moment of intensity (I_s) against s in Fig. 1. The good orientation of the sample restricted the degree of slit smearing to an acceptable level. However, the degree of misorientation which is present would interfere with the drawing of any precise quantitative deductions from the data, not only on account of slit smearing but also because it would tend to invalidate the use of the relation $I_{(s)}.s$ for the total diffracted intensity at s. Higher precision could only be obtained by destroying the texture of the sample, correcting the pattern for slit smearing and expressing the total diffracted intensity at s as $I_{(s)}.s^2$.

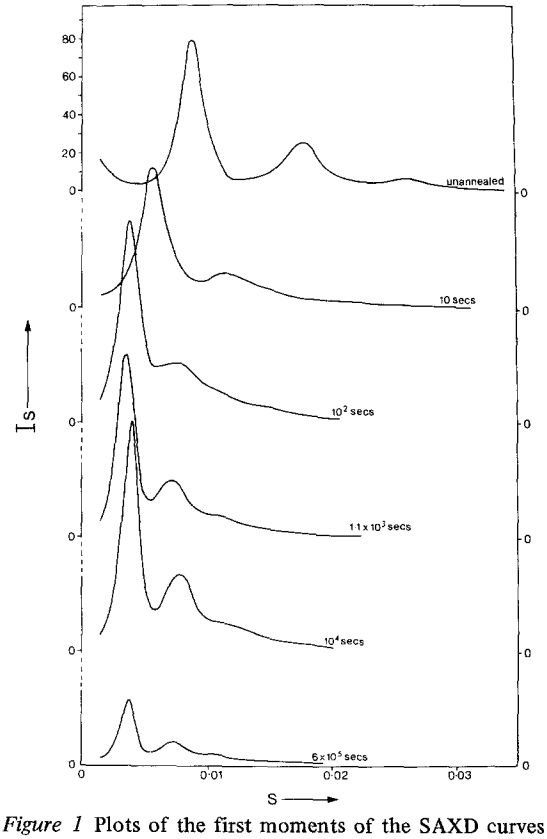

Figure 1 Plots of the first moments of the SAXD curves for the as-crystallized specimen and those annealed at 125° C for the times indicated.

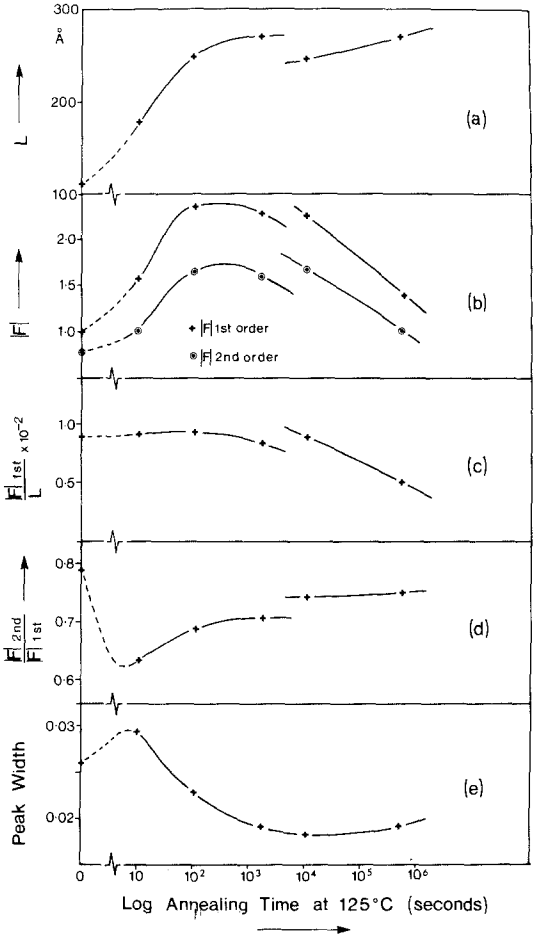

Figure 2 Parameters measured from the SAXD curves plotted against log annealing time. (a) The long period; (b) the normalized structure factors of the first and second order peaks which give an indication of the change in integral electron deficiency in each long period on annealing; (c) the normalized structure factor for the first order peak divided by the long period. This parameter is related to the total electron deficiency in all the fold surfaces; (d) the ratio of the structure factors of the first and second order peaks; (e) the integral width of the first order peak.

The long period increases rapidly during the first 100 sec at 125° C from 111 Å to 252 Å. Whereas after much longer annealing times it never increases above 272 Å. The long period is plotted against log annealing time in Fig. 2a. The discontinuity between 1.1×10^3 and 10^4 sec probably reflects a change in annealing procedure (cf. Section 3.1). Peaks representing second order diffraction from the long period were visible at all stages of annealing although they were less well-defined after short annealing periods.

There is no evidence for superposition of patterns representing different long periods.

In order to further characterize the changes in SAXD on annealing, relative structure factors for the first and second order peaks from all the specimens were calculated by a method described by Strobl [21] and Strobl and Müller [22] but with their relation modified as below to account for the preferred orientation of our specimens:

$$|F|^2 \propto L^2 \int_{s=\frac{l+\frac{1}{2}}{L}}^{\frac{l-\frac{1}{2}}{L}} I_{(s)} s . \mathrm{d}s$$

where l is the order of the reflection and L the long period.

The integral electron deficiency in each long period is given by $|F|_0$ which it is not possible to measure. The structure factor of the first low angle reflection, $|F|_{1st}$, will also depend on the integral electron deficiency varying linearly with $|F|_0$; in addition however, it is sensitive to the distribution of the electron deficiency within the long period. On the premise that the electron deficient regions are centred at the interface between adjacent crystals, then an increase in the thickness of these regions in [0 0 1] so that they occupy a greater proportion of the long period but without any change in the integral electron deficiency will result in a decrease in $|F|_{1st}$. As well as varying linearly with $|F|_0$ like $|F|_{1st}$, $|F|_{2nd}$ is also dependent on the mean thickness of the electron deficient regions but will respond more rapidly to changes in this parameter. For example as the mean thickness of the deficient regions increases from zero to one half of the long period, $|F|_{2nd}$ decreases from a value equal to $|F|_{1st}$ to zero. It follows, therefore, that any changes in $|F|_{1st}$ as the result of annealing which are exactly mirrored by proportional changes in $|F|_{2nd}$, are due to changes in the integral electron deficiency within each long period. Variations in the ratio $|F|_{2nd}/|F|_{1st}$ will indicate changes in the thickness of the deficient layers expressed as a fraction of the long period.

The results of the structure factor measurements are summarized in Fig. 2b, all structure factors being normalized to $|F|_{1st} = 1.0$ for the unannealed specimen. The fact that both $|F|_{1st}$ and $|F|_{2nd}$ follow the same trends during annealing, namely an increase over the first 100 sec at 25° C, then fairly constant up to 10^4 sec and finally a marked reduction after 6×10^5 sec suggests that the bulk of the changes can be accounted for by variations in the integral electron deficiency in each long period. The initial increase in the structure factors corresponds to the stage at which the long period is increasing most rapidly. Fig. 2c, in which $|F|_{1st}/L$ is plotted against annealing time, illustrates that up to 10^4 sec the increase in integral electron deficiency in each long period is balanced by the increase in long period itself. Thus, as the crystals thicken there is an increase in electron deficiency per crystal, but little change in the sum of the electron deficiencies associated with all the fold surfaces in the sample. The reduction in both structure factors after annealing for 6×10^5 sec may represent either an increase in the degree of order and hence density near to the fold surfaces or some degree of oxygen degradation which could reduce the electron deficiency in the defect regions. Either explanation would also be in accord with the substantially higher overall density of this sample (Table I).

If the ratio $|F|_{2nd}/|F|_{1st}$ were to remain exactly constant as the long period increased during annealing, it would imply that the thickness of the electron deficient region increased in proportion to the long period. The observation (Fig. 2d) that the ratio for the unannealed crystal is decreased in the early stages of annealing, indicates that this treatment in addition to rapidly increasing the long period, spreads the electron deficient region over a greater proportion of the long period.

The integral peak widths were also measured for the first order low angle peak and are plotted in Fig. 2e. The peak width, after an initial increase for the 10 sec anneal, generally decreases as the annealing time is lengthened.

4.2. SAXD – some conclusions

The changes in SAXD on annealing reported in the previous section show no really new effects. For example, the increase in intensity of the first and second order peaks on annealing is a well-estab-

lished phenomenon and the decrease in relative intensity of the second order peak in the early stages of annealing was noted by Statton in 1961 [4]. The main purpose of presenting this semi-quantitative data is to provide as full a background as possible against which the wide angle results can be discussed (Section 5). It does however, permit several conclusions to be drawn about the annealing process which will assist in the interpretation of the 0 0 2 peak profiles.

(a) There is no evidence for the superposition of SAXD patterns corresponding to significantly different long periods and there is a clearly recognizable long period at all stages of annealing. It follows that each crystal entity increases in thickness at much the same rate and it is unlikely that annealing causes the complete melting of the original crystals and the growth of a new phase containing crystals with a new long period. It is also very difficult to envisage the increase in long period as being the result of chain interpenetration into adjacent crystals leading to the annihilation of the fold surfaces, for in order to preserve sufficient order in the crystal superlattice commensurate with the clear low-angle diffraction peaks observed, either every second or every third fold surface would have to be systematically preserved.

(b) The increase in crystalline thickness on annealing is not reflected in an overall increase in the thickness of the oriented specimen. The implication of this observation is that there must be some localized movement of crystals or parts of crystals in the direction perpendicular to the molecular chains during annealing.

(c) For annealing at 125° C the long period obtained after 100 sec is at least 90% of that reached after very much longer times.

(d) The integral electron deficiency in each long period as indicated by the structure factors of the first and second order peaks increases linearly with the long period to a maximum in the range 10^2 to 10^4 sec. It decreases markedly at longer times.

(e) Trends in the ratio of $|F|_{2nd}/|F|_{1st}$ are an indication of the effect of annealing on the proportion of long period occupied by the electron deficient region. The proportion was found to increase rapidly in the initial stages of annealing but then decreased as the time at 125° C was extended. Even at the longest time however, the extent of the density deficient region as a proportion of the long period exceeded that for the unannealed material.

5. Analysis of the 0 0 2 diffraction peak

5.1. Introduction and preview of results

The technique of analysis of the 0 0 2 peak in terms of the intensity of the subsidiary maxima and also its corrected correlation function has already been described for the case of the unannealed specimen [20]. The greater thickness of crystallites in the annealed specimen means that the 0 0 2 peak is correspondingly sharper and hence the smearing effects of slit and spectral widths more significant. It is therefore very necessary to deconvolute the experimental broadening using Stoke's method [23] and use either the correlation function or the reconstituted peak as the basis for microstructural predictions.

The salient features of the correlation function of the annealed specimen together with the form of the corrected reconstituted peak will be illustrated in detail for the sample annealed for 1.1×10^3 sec at 125° C.

The corrected correlation function of the 0 0 2 peak for this sample is drawn in Fig. 3. The negative curvature around the origin is of approximately the same extent as for the unannealed sample, but the region of positive curvature is broken up into a series of nearly linear segments separated by comparatively rapid changes of slope. A plot of the second derivative of the function in Fig. 4a illustrates the effect clearly. Because this particular form of correlation function will be of considerable significance as far as structural analysis is concerned it is useful to check that the segmentation is not an artefact introduced by the correction of the experimental peak. Fig. 4b shows the curvature of the correlation function before correction. The same periodicity is apparent although as one would expect it is not as sharply defined as in the case of the corrected function. It is also difficult to see how the segmented correlation function could be the result of a termination error in the original data, as these were collected over a sufficiently wide range of 2θ to include both extremities of the peak. Furthermore, the peak reconstituted from the corrected correlation function (Fig. 5) shows no evidence of premature termination. This reconsituted peak is also of interest because it shows subsidiaries which were smeared beyond recognition in the experimental data. The form of the subsidiaries however, differs considerably from those observed on the 0 0 2 peak of the unannealed material [20]. Their width is considerably less than one half of the

spacing of the first two minima, and the main peak slopes down to these minima much more gradually than for the unannealed case. The profile of the reconstituted peak apparently reflects the unusual features of the correlation function.

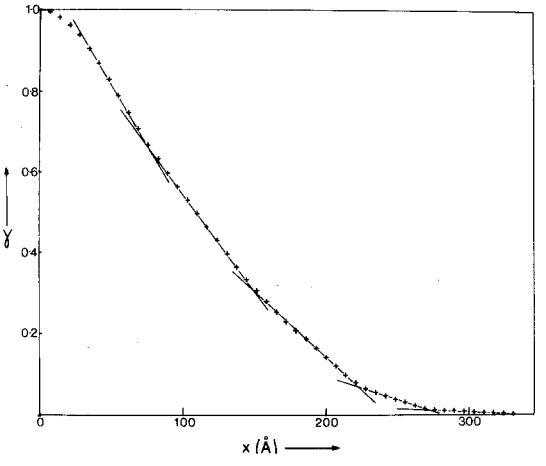

Figure 3 The corrected correlation function for the 0 0 2 peak of the specimen annealed for 1.1×10^3 sec at 125° C. The function is only plotted for positive values of x.

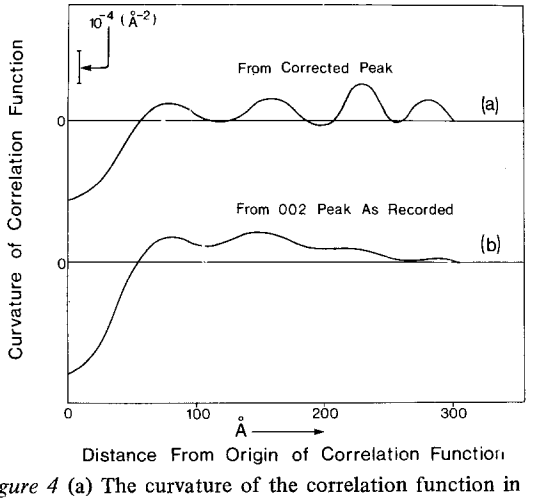

Figure 4 (a) The curvature of the correlation function in Fig. 3. (b) The curvature of the same function, but before it had been corrected for experimental broadening.

5.2. Results and their interpretation

Fig. 6 is a plot of the curvatures of the correlation functions of both the as-crystallized and annealed samples. It can be seen that, with the exceptions of the unannealed specimen and that annealed for the longest time (6×10^5 sec), the functions are clearly segmented.

The segmented nature of the correlation function indicates that straight sections of polymer chains (known as stems) which form the crystal

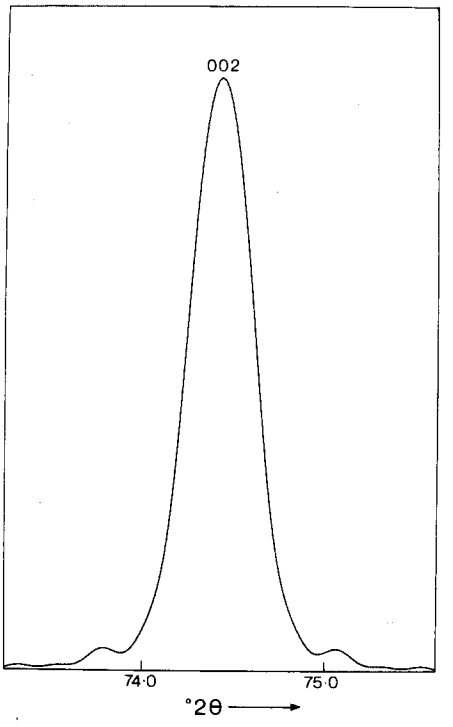

Figure 5 The 0 0 2 diffraction peak of the sample annealed for 1.1×10^3 sec at 125° C reconstituted from the corrected correlation function of Fig. 3.

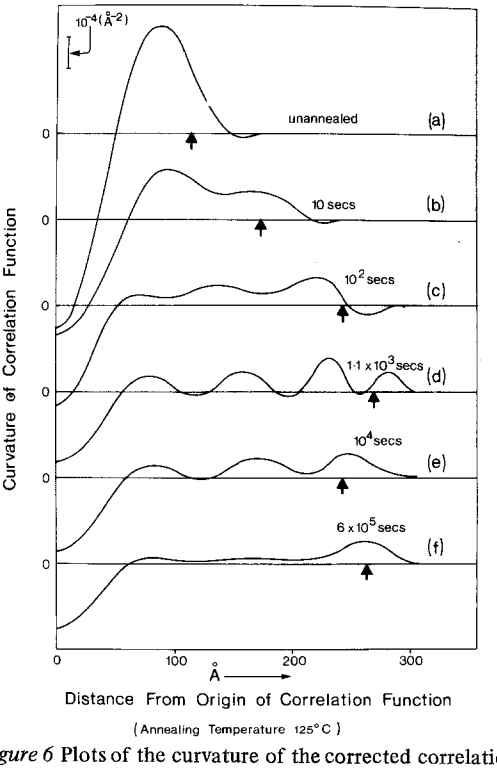

Figure 6 Plots of the curvature of the corrected correlation functions for the samples annealed for different periods at 125° C. The arrow marks on the distance axis represent the long period as measured by SAXD.

have certain preferred lengths and it appears that these preferred lengths are multiples of a unit stem length. There is a variety of ways in which the various preferred stem lengths may be dispersed throughout the crystals and the specimen. But, as far as the profile of the 0 0 2 peak is concerned there are two distinct types of distribution: (1) within any coherently defecting domain of the crystal the chain stems are all of the same preferred length; (2) the various preferred stem lengths are proportionally represented in each of the coherently diffracting domains.

It must also be assumed for both (1) and (2) that the stems terminate within definable planar regions parallel to the 0 0 2 planes, and that the thickness of these regions (analogous to the transition regions at the fold surfaces of the unannealed crystals [20]) is less than one half of the unit stem length. If this were not the case, segmented correlation functions would not be observed.

Although distributions (1) and (2) will affect the 0 0 2 peak profile in different ways, it is not possible, without independent knowledge of the proportions of the various preferred stem lengths present, to determine uniquely which of the two distributions is correct.

However, in view of the other structural data available, especially those from SAXD measurements, it is worthwhile to analyse the 0 0 2 peak and its segmented correlation function on the basis of each of the limiting types of distribution in turn.

5.2.1. *Analysis for distribution (1) (stems distributed so that all those in any one coherently diffraction domain are of the same preferred length)*

The analysis due to Warren and Averbach [24] is appropriate in this case. They showed that the positive curvature of the correlation function was proportional to the number distribution function describing the range of crystalline sizes. Their treatment was for "square" crystal shaped functions and can only be applied to these results if the region of the correlation functions with negative curvature is ignored, see Fig. 6. However, by taking into account the possibility of a trapezium-shaped profile with the crystalline perfection decreasing to zero over a finite distance in the region of the fold surface, we can explain the observation that the negative curvature of the correlation function is not confined to the origin and that the regions of positive curvature representing preferred stem lengths are spread over a significant range. It is possible, however, that some of the negative curvature may be the result of underestimation of the intensity in the tails of the 0 0 2 peak, and that correspondingly, the spread of the regions of positive curvature reflects a genuine dispersion in the stem lengths around the preferred value.

On the basis of this analysis, it can be said that the preferred stem lengths are multiples of a unit stem length, and that the relative proportions of domains of different stem length can be gauged from the areas under the corresponding "peaks" of the curvature plots (Fig. 6).

5.2.2. *Analysis for distribution (2) (stems distributed so that there is a representative sample of preferred lengths within any coherently diffracting domain)*

On the assumption that the crystal profile is identical for each diffracting domain, the segmented correlation function must represent the autoconvolution of a stepped crystal profile function. The form of the stepped profile which would be responsible for the observed correlation functions can be calculated if three assumptions are made:

(a) The crystal profile consists of steps of equal width.

(b) The gradual change in slope between the segments of the experimental function reflects the fact that the steps of the crystal profile are not infinitely steep.

(c) If the experimental correlation function is modified by extrapolation of adjacent segments until they intercept; then, the new function corresponds to a crystal profile similar to that responsible for the experimental function, except in that the step rises are infinitely steep.

The relationship between the height of the steps of the profile and the position of the sharp changes in slope of its correlation function is given by (for a three-step profile):

$$ac = kA$$

(represents the point during autoconvolution at which the two identical profiles overlap by one step width)

$$ab + bc = kB$$

(overlap of two step widths)

$$a^2 + b^2 + c^2 = kC$$

(complete superposition).

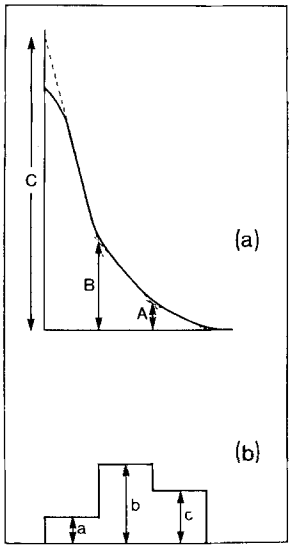

Figure 7 Definition of the parameters used for the calculation of the stepped crystal profiles form the segmented correlation functions. (a) Segmented correlation function; (b) stepped crystal profile.

The terms are defined in Fig. 7, (except k which is a constant of proportionality).

In the case of the specimen annealed for 1.1×10^3 sec at 125° C, the correlation functions shows four segments and it is analysed in terms of a profile with four steps; the relationship in this case being:

$$ad = kA$$

$$ac + bd = kB$$

$$ab + bc + cd = kC$$

$$a^2 + b^2 + c^2 + d^2 = kD.$$

The profiles determined for the annealed samples by the solution of these relations are shown in Fig. 8.

A computer program has been written to numerically autoconvolute the crystal profile and compare the resultant correlation functions with those obtained directly. This, in addition to checking the profiles determined analytically, has enabled the correlation functions to be determined for profiles in which the steps are not infinitely steep. Such functions resemble more closely those determined experimentally, having negative curvature extending from the origin and a more gradual change in slope between the segments. A good fit was obtained with the experimental functions for the case where all changes in height between the steps of the profile occurred over a distance of 30 Å. This value is of the same order as the thickness of the transition region at the fold surfaces measured for unannealed crystals [20]. The introduction of transition regions into the stepped profile does not significantly affect the position of the changes in slope on the correlation function (as defined in Fig. 7), apparently justifying assumptions (b) and (c) above.

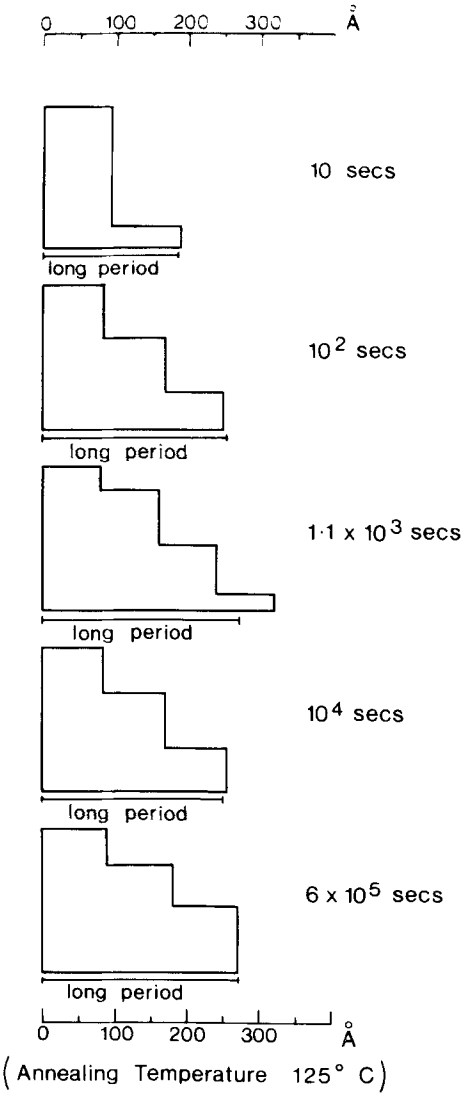

Figure 8 Stepped crystal profiles (for [0 0 1] direction) calculated from the correlation functions of the specimens annealed at 125° C. The bars under each of the profiles represent the long period (to the same scale) as measured by SAXD.

5.3. Discussion of the analysis of the 002 peak profile in relation to the SAXD data

Whichever of the two interpretations of the correlation function is to be chosen, its segmented

form indicates that particlular chain stem lengths within the chain-folded crystal are preferred; the more detailed analyses (1 and 2) in Section 5.2 are approaches to describe the positioning of the various preferred stem lengths within the crystals and throughout the sample. The preferred lengths are multiples of about 80 Å which compares with the value of 85 Å for the "mean" crystallite thickness in the unannealed material [20] but is significantly less than the long period of 111 Å. There appears, however, to be a small increase in the unit stem length as the annealing time is increased from 100 sec to 6×10^5 sec.

The discontinuity apparent in the low-angle data between the annealing times of 1.1×10^3 and 10^4 sec and attributed to the difference in annealing procedure (Section 3.1) is also apparent in the plots of the curvature of the correlation function (Fig. 6). At 1.1×10^3 sec there is evidence of doubling, trebling and quadrupling of the unit stem length, whereas at 10^4 and 6×10^5 sec there is no sign of quadrupling. In addition, the unit stem length of the 10^4 sec sample is about 9 Å greater than in that annealed for 1.1×10^3 sec and the various preferred stem lengths are not as clearly defined. The discontinuity although spoiling the otherwise smooth development of multiples of the unit stem length does nevertheless illustrate the complementary nature of both low- and wide-angle data.

There are two possible mechanisms which can explain the thickening of crystallites as multiples of their original chain length. The first is the unlooping mechanism put forward by Dreyfuss and Keller [15] to account for the observed doubling and quadrupling of the long period of polyamides as the result of annealing (Fig. 9a). The operation of this mechanism leads inevitably to crystal thicknesses which are multiples of the original. Another mechanism which does not depend on the chain unlooping, but does not preclude it, can be envisaged if crystals only thicken as space becomes available to accommodate them. The thickness increments of the crystals are then determined by the extent (in the chain direction) of voids within adjacent crystals. It is not unreasonable to expect that such voids will extend across the full thickness of the crystals and that the increments will, therefore, be similar to the original crystal thickness (Fig. 9b). The unlooping mechanism of Dreyfuss and Keller does, however, have the additional attraction that its operation above 117° C could provide an explanation of the change in annealing behaviour observed by Bair *et al.* [12] and Blackadder and Lewell [17] at that temperature.

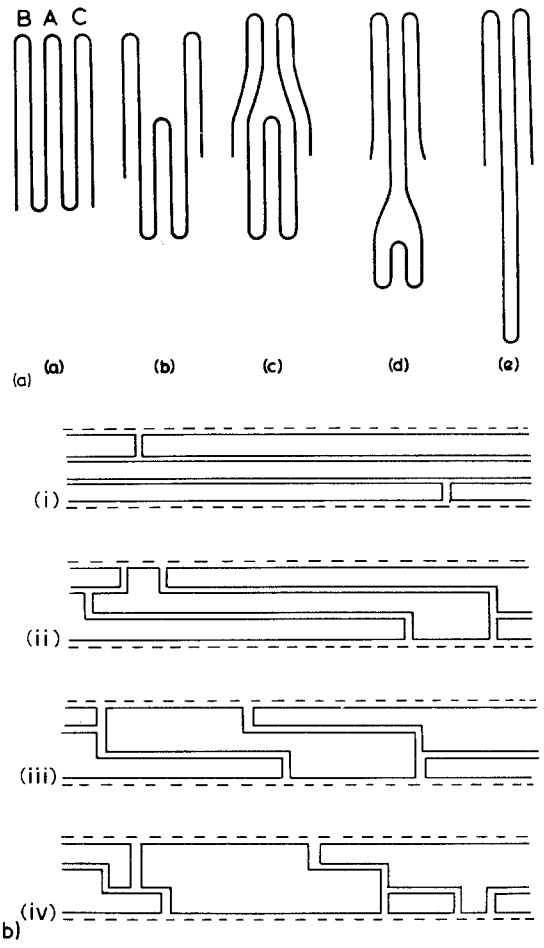

Figure 9 Mechanisms which could account for the preferred stem lengths observed in the annealed crystals; (a) unlooping mechanism of Dreyfuss and Keller [15]; (b) a sequence showing how multiple thicknesses can result from interpenetration of regions of adjacent crystals.

Each of the two alternative interpretations of the experimental correlation functions will now be considered in the light of the SAXD data.

5.3.1. Interpretation (1)

The existence of a single well-defined long period as shown by the SAXD pattern indicates that the stacks of parallel crystallites each have the same long period. Also, the fact that the long period is of the order of the largest crystallite thickness in the distribution function measured from the 0 0 2 peak rules out the possibility that single, double or treble thickness crystallites are arranged in random order in the stacks, for although a single long

period would be identifiable from the SAXD pattern it would have much the same value as the unit crystal thickness. It is difficult, therefore, to relate the SAXD information to a periodic size distribution. We have either to say that only a fraction of the crystallites are regularly stacked and responsible for the SAXD reflection and that it is this fraction alone which treble in thickness (or quadruple for the 1.1×10^3 sec anneal), with the crystallites not in the regular stack remaining single or only doubling in thickness, (Fig. 10a); or, that any given crystallite consists of single, double or treble thickness regions which scatter incoherently in terms of the 0 0 2 peak and that the treble (or maximum thickness region) determines the long period (Fig. 10b). The arrangement of the treble thickness crystallite only in the stacks is strictly possible although unlikely especially as the preferred orientation of the crystallites as revealed by both SAXD and wide angle transmission photographs is comparable. For the division of each crystallite into region of unit, double and treble thickness however, it is necessary to assume that the areas above the thinner regions are filled with material which is in some way disordered so that it does not scatter coherently into the 0 0 2 peak, otherwise the density defect would far exceed that observed experimentally. This arrangement is certainly feasible and would account for both low- and wide-angle X-ray data. Presumably the molecules forming the extra disordered material would have belonged to the unannealed crystallites, and it is neater to consider the whole crystal as trebling in thickness but some of the newly extended regions perhaps failing to crystallize. This interpretation is based on the assumption that the regions of a crystal which are of different thickness should not scatter coherently. Their lateral extent must therefore exceed the size of the coherently diffracting domains for that direction which can be estimated to be about 200 Å from the width of the 1 1 0 and 2 0 0 diffraction peaks.

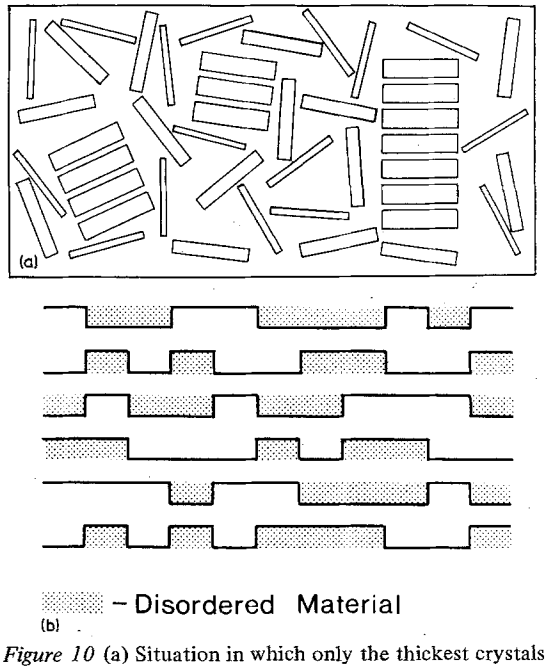

Figure 10 (a) Situation in which only the thickest crystals are arranged in regular stacks (see text). (b) Stacks of crystals consisting of regions of unit, double and treble thickness which diffract independently into the 0 0 2 peak.

One particular problem with this model is that it is difficult to see any reason why various regions of the same crystal which we presume are large enough to be representative should behave so differently during annealing. The problem is emphasized by the correlation function of the sample annealed for 10 sec at 125° C which shows evidence of doubling but not trebling of the unit thickness, the thickness of the double entity corresponding approximately to the long period. The implication of this is that the separate regions of the crystal which thicken do so in one and the same direction, and this apparently corporate behaviour must be reconciled with the fact that other perhaps intervening regions do not thicken at all.

5.3.2. Interpretation (2)

The stepped crystal profiles (Fig. 8) imply that within a domain which is coherently diffracting into the 0 0 2 peak, there is a discontinuous variation in diffraction efficiency between layers which are parallel to the fold surfaces and each of a thickness comparable to that of the unannealed crystallites.

The lower diffraction efficiency of some layers could be the result of voids, a generally high density of defects, or of defects so arranged that some otherwise crystalline material in these layers scatters X-rays out of phase with the diffraction from the main crystal. It is surprising that all these stepped profiles derived from the correlation functions are asymmetric which, if one equates the layers of lower diffraction efficiency with those added during the thickening process, suggests that during annealing the crystals thicken in one direction only. Thus, on the basis of stepped crystal profiles we have evidence for asymmetric thickening; a process which has already been suggested to explain the

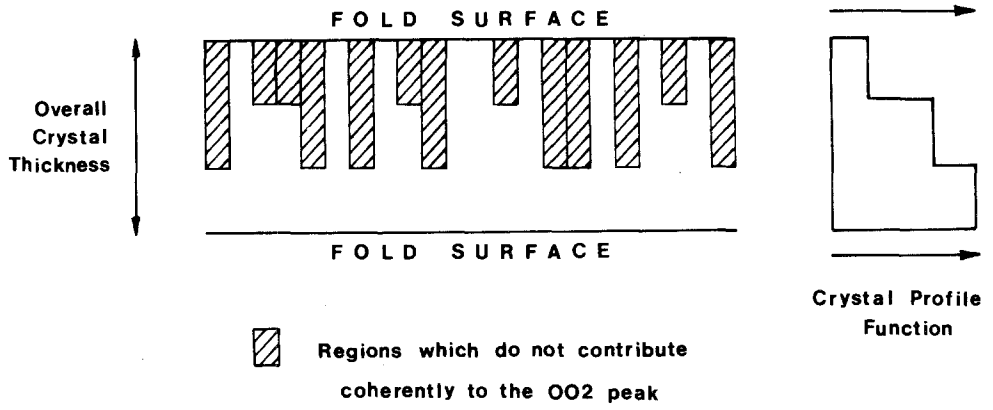

Figure 11 A model of a thickened crystal corresponding to the stepped crystal profiles determined from the correlation functions. The whole crystal as drawn is assumed to diffract coherently.

observation of crystals which have doubled but not trebled in thickness.

We suggest that interpretation 2 is the more realistic. It is completely compatible with the SAXD data and, taking the layers of lower diffracting efficiency as being at least partly disordered, provides an explanation of the observed increase in both the integral electron deficiency in each long period and the extent of the electron-deficient region observed after anneals of between 10 and 10^4 sec, which does not entail the generation of additional defect material between the fold surfaces. The asymmetric thickening also explains the observation of crystals which have doubled but not trebled in thickness. A structural model in accord with the SAXD results and interpretation (2) of the 0 0 2 peak profile is sketched in Fig. 11.

6. Conclusions

(1) There are no observable changes in the preferred orientation of the sample as a result of annealing at 125° C. This applies to both small- and wide-angle diffraction data.

(2) Each of the crystallite entities contributing to the SAXD pattern increases in thickness at the same rate on annealing.

(3) Annealing does not change the dimensions of the oriented sample which indicates that some at least of the thickening crystallites must move sideways to compensate for their growth in the chain direction.

(4) The integral electron deficiency in each long period increases linearly with the long period to a maximum in the range 10^2 to 10^4 sec. It decreases markedly at longer times.

(5) The extent of the electron-deficient region expressed as a fraction of the long period increases rapidly after short anneals and then gradually decreases with increasing time at 125° C.

(6) After annealing there is evidence for preferred chain stem lengths which are multiples of a unit length. The unit length is similar to the mean stem length of the unannnealed crystals.

(7) Each crystal contains a representative selection of the preferred stem lengths.

(8) If it is assumed that each coherently diffracting domain contains representative stem lengths, then the arrangement of the stems in the crystal leads to an asymmetric stepped profile.

(9) The implication of the asymmetric profile is that the crystal thickens preferentially in one direction only.

Acknowledgements

This work was started at the instigation of Professor Keller and has continued with his constant encouragement and guidance. Some of the experimental work was carried out during a period spent at the H. H. Wills Physics Laboratory at Bristol University. The author is also indebted to Dr Y. Kobayashi for his preparation of the solution-grown mats, and to Professor F. C. Frank, Dr E. Atkins, Dr M. Folkes, and Dr D. Saddler for stimulating discussions and helpful suggestions. Mr F. Huggins provided invaluable assistance with the preparation of the artwork and the construction of the low-angle camera.

References

1. A. KELLER, *Phil. Mag.* 2 (1957) 1171.
2. E. W. FISCHER, *Z. Naturforsche* **12a** (1957) 753.
3. A. KELLER and A. O'CONNER, *Discuss. Faraday Soc.* 25 (1958) 114.
4. W. O. STATTON, *J. Appl. Phys.* 32 (1961) 2332.
5. F. J. BALTA CALLEJA, D. C. BASSETT and

A. KELLER, *Polymer* **4** (1963) 269.
6. W. O. STATTON and P. H. GEIL, *J. Appl. Polymer Sci.* **3** (1960) 357.
7. H. NAGAI and N. KAJIKAWAWA, *Polymer* **9** (1968) 177.
8. RYONG-JOON ROE, C. GIENIEWSKI and R. G. VADIMSKI, *J. Polymer Sci.* **11** (1973) 1653.
9. K. M. SINNOTT, *J. Appl. Phys.* **37** (1966) 3385.
10. P. N. LOWELL and N. G. MCCRUM, *Polymer Letters* **5** (1967) 1145.
11. L. MANDELKERN and A. L. ALLAN, *J. Polymer Sci.* **134** (1966) 447.
12. H. E. BAIR, R. SALOVEY and T. W. HUSEBY, *Polymer* **8** (1967) 9.
13. D. H. RENEKER, *J. Polymer Sci.* **59** (1962) 39.
14. A. PETERLIN, *Polymer* **6** (1965) 25.
15. P. DREYFUSS and A. KELLER, *Polymer Letters* **8** (1970) 253.
16. E. W. FISCHER and G. F. SCHMIDT, *Angew Chem.* **74** (1962) 551.
17. D. A. BLACKADDER and P. A. LEWELL, *Polymer* **11** (1970) 147.
18. W. O. STATTON, in "Newer Methods of Polymer Characterisation", edited by B. Ke (Interscience, New York, 1964) Ch. 6.
19. Y. KOBAYASHI and A. KELLER, *J. Mater. Sci.* **9** (1974) 2056.
20. A. H. WINDLE, *J. Mater. Sci.* **10** (1975) 252.
21. G. R. STROBL, *J. Appl. Cryst.* **6** (1973) 365.
22. G. R. STROBL and N. MÜLLER, *J. Polymer Sci.* **11** (1973) 1219.
23. A. R. STOKES, *Proc. Phys. Soc. (London)* **A61** (1948) 382.
24. B. E. WARREN and B. L. AVERBACH, *J. Appl. Phys.* **21** (1950) 595.

Received 7 February and accepted 8 May 1975.